



Photoinduced current and emission induced by current in a nanowire transistor: Temperature dependence

MAHVASH ARABI DAREHDOR* and NASSER SHAHTAHMASSEBI

Department of Physics and Nanocentre Research, Ferdowsi University of Mashhad, Mashhad, Iran

*Corresponding author. E-mail: mahvasharabi64@yahoo.com

MS received 17 March 2014; revised 24 November 2014; accepted 12 January 2015

DOI: 10.1007/s12043-015-1033-5; ePublication: 6 October 2015

Abstract. In this paper, we present a theoretical study on a light emitting and current carrying nanosystem, in the nonzero temperature regime. The system under consideration is a semiconducting nanowire sandwiched between two semi-infinite metallic electrodes. The study was performed using the Keldysh nonequilibrium Green's function method. We systematically investigate the photoinduced current and the light emission induced by this electronic current in the presence of gate voltage. The temperature dependence of these processes are also investigated in the temperature range of 3–300 K. Our study shows that, the photoinduced current is due to the transfer of electrons from highest occupied molecular orbital (HOMO) to the lowest unoccupied molecular orbital (LUMO). Thus, the separation of electron from the electron–hole pair creates a free electron which is responsible for the observed photoinduced current. The same conclusion is also arrived at for the reverse process of light emission under the influence of the electronic current.

Keywords. Keldysh nonequilibrium Green's function method; nanowire; temperature dependence; photoinduced current; light emission.

PACS Nos 73.63.–b; 78.67.–n; 78

1. Introduction

In recent years, there has been much progress in the field of nanoelectronics and nanooptics. There are already a large number of experimental and theoretical works on the electronic current induced by light emission and vice versa. It has been shown that, band-gap excitations in TiO₂ nanoparticles and nanotubes, lead to the injection of electrons to the conducting channel, resulting in the generation of photocurrent in a photoelectrochemical solar cell. Similar studies on the conducting polymers showed that, photoinduced electron transfer from the excited state of a buckminsterfullerene, C₆₀, was possible [1]. In conventional electronics, charge carriers are electrons or holes. But in light emitting diodes (LEDs) both electrons and holes are charge carriers and they are responsible for

the conductivity. Due to the Coulomb interaction between electrons and holes, excitons create and recombination of these excitons results in the emission of light. In the reverse process, the incidence of light on a nanosystem may cause the flow of electrical current.

Several researchers [2–5] have studied the mechanisms of optical and electrical transport in LEDs, and also nanowires [2–5]. As examples, we can mention the design of LEDs and ZnO nanowire (NW) field-effect transistors in which the photoinduced electrons are produced by laser irradiation [6]. Jeong *et al* made a device in which electroluminescence with long wavelength was observed [7]. There are also a large number of theoretical and numerical works on such systems, where the current excites the system to produce light. Among the theoretical approaches, the Keldysh method is more suitable for studying excited systems, because in this case the system under study is being excited by the incident light. The Keldysh method employs the Green's function and the self-energies of the system to study the transport properties of nanosystems.

In this work, we present a study on the transport properties and the light emission in a system of a semiconducting nanowire sandwiched between two metallic electrodes in the presence of gate voltage. The paper is arranged as follows: In §2, we introduce our model and the details of the method of nonequilibrium Green's function (NEGF) and the calculation of the transport properties of the model system. Section 3 is devoted to the optical flux (fluorescence) and the derivation of I_{em} , the light emission induced by the electronic current. In §4, the electronic source-drain current I_{sd} is derived using the Keldysh formalism and we study the behaviour of the transport and optical properties of the system vs. the temperature, gate voltage and the bias voltage. Finally, the conclusion and the discussion of our results are presented in §5.

2. The model and the method

We perform our studies for a system consisting of electrode/molecule/electrode in which the molecule is assumed to be a nanowire with two energy levels. These two levels are taken to be the HOMO and LUMO of the molecule which are shown by $|1\rangle$ and $|2\rangle$ respectively. The electrodes are to be semi-infinite metallic and are characterized by their chemical potentials μ_L and μ_R , where R and L stand for the right and left electrode, respectively. The bias voltage is V , where $\mu_L - \mu_R = eV$. The Hamiltonian of this system is, therefore, given by [8]

$$\hat{H} = \hat{H}_0 + \hat{V}, \quad (1)$$

$$\hat{H}_0 = \sum_{m=1,2} \varepsilon_m \hat{c}_m^+ \hat{c}_m + \sum_{k \in \{L,R\}} \varepsilon_k \hat{c}_k^+ \hat{c}_k + \hbar \sum_{\alpha} \omega_{\alpha} \hat{a}_{\alpha}^+ \hat{a}_{\alpha}. \quad (2)$$

The Hamiltonian H_0 consists of three parts. The first term is the Hamiltonian for isolated nanowire, while the second and third terms are the Hamiltonians for the electrodes and the radiation field, respectively. The operators \hat{c} and \hat{c}^+ refer to annihilation and creation operators of one electron, and \hat{a} and \hat{a}^+ denote the annihilation and creation operators of

photons, respectively. In eq. (1), \hat{V} denotes the excitation potential or the coupling and we consider it to be the sum of three components V_M , V_N and V_P as follows:

$$\hat{V} = \hat{V}_M + \hat{V}_P + \hat{V}_N \quad (3)$$

$$\hat{V}_M = \sum_{K=L,R} \sum_{m=1,2; k \in K} \left(V_{km}^{(MK)} \hat{c}_k^+ \hat{c}_m + \text{h.c.} \right), \quad (4)$$

$$\hat{V}_P = \left(V_0^{(P)} \hat{a}_0 \hat{c}_2^+ \hat{c}_1 + \text{h.c.} \right) + \sum_{\alpha \neq 0} \left(V_\alpha^{(P)} \hat{a}_\alpha \hat{c}_2^+ \hat{c}_1 + \text{h.c.} \right), \quad (5)$$

$$V_N = \sum_{K=L,R} \sum_{k \neq k' \in K} \left(V_{kk'}^{(NK)} \hat{c}_k^+ \hat{c}_{k'} \hat{c}_2^+ \hat{c}_1 + \text{h.c.} \right). \quad (6)$$

In these equations, V_M describes the electron transfer between the nanowire and the electrodes, leading to the current. V_N is the energy transfer between the electrons of the nanowire and electron–hole excitation of the electrodes and V_P is the molecule–radiation field coupling, i.e., it represents the energy transfer from photons to the electrons in the nanowire. In V_N , c_1 and c_2^+ show annihilation of electron in the state $|1\rangle$ and creation of an electron in the state $|2\rangle$ of the nanowire, respectively. $c_{k'}$ and c_k^+ represent annihilation of electron in k' state and creation in k state of the electrodes, respectively. The transition of the electron from k to k' in the electrode would result in the transfer of energy to the nanowire and transition of electron from $|1\rangle$ to $|2\rangle$.

In the above equations we have explicitly written the term corresponding to mode ‘0’ that pumps the system. With regard to optical processes, we limit ourselves to near-resonance processes pertaining to linear spectroscopy. This implies that the back effect of the electronic system on the radiation field is disregarded and justifies the use of the rotating wave approximation (RWA) in eq. (5). Also for this reason we may consider only zero- and one-photon states of the radiation field, taking $V_0^{(P)}$ (but not $V_{\alpha \neq 0}^{(P)}$) to be proportional to the incident field amplitude ε_0 , and treat all processes up to second-order in this coupling. We note that all $V_\alpha^{(P)}$ coefficients reflect the properties of the local electromagnetic field at the molecular bridge which in turn, depend on the metallic boundary conditions. By applying a gate voltage, the same amount of voltage is added to the diagonal elements of the Hamiltonian [9].

In the Keldysh nonequilibrium Green’s function (NEGF), the current of process B is derived using the Green’s function and self-energies

$$I_B = \int_{-\infty}^{+\infty} \frac{dE}{2\pi\hbar} \text{Tr} \left[\Sigma_B^<(E) G^>(E) - \Sigma_B^>(E) G^<(E) \right], \quad (7)$$

where the Green’s functions are propagators. The equation for the current flowing between two electrodes with a molecule located between them, eq. (7), was first derived by Langreth [10]. In the first step, by neglecting the radiative coupling V_P and the nonradiative energy transfer V_N , the Hamiltonian becomes

$$\hat{H}_0 = \hat{H}_0 + \hat{V}_M. \quad (8)$$

This Hamiltonian consists of one-particle operators. We set the retarded and advanced self-energies purely imaginary and energy independent in the wide band approximation. Thus, the self-energies become diagonal in the 1-2 representation.

$$\Sigma_{MK}^r = (\Sigma_{MK}^a)^* = \begin{pmatrix} -i\Gamma_{MK,1}/2 & 0 \\ 0 & -i\Gamma_{MK,2}/2 \end{pmatrix}, \quad (9)$$

where K = L, R refer to the left and right electrodes, respectively. Using these self-energies the retarded and advanced Green's functions become

$$G^r(E) = \begin{pmatrix} \frac{1}{E - \varepsilon_1 + i\Gamma_{M,1}/2} & 0 \\ 0 & \frac{1}{E - \varepsilon_2 + i\Gamma_{M,2}/2} \end{pmatrix}; \quad G^a(E) = [G^r(E)]^*, \quad (10)$$

where $\Gamma_{M,m} = \Gamma_{ML,m} + \Gamma_{MR,m}$; $m = 1, 2$ and the lesser and greater self-energies are defined as follows;

$$\Sigma_M^{>,<} = \Sigma_{ML}^{>,<} + \Sigma_{MR}^{>,<}, \quad (11a)$$

$$\Sigma_{MK}^{<}(E) = \begin{pmatrix} if_K(E)\Gamma_{MK,1} & 0 \\ 0 & if_K(E)\Gamma_{MK,2} \end{pmatrix}, \quad (11b)$$

$$\Sigma_{MK}^{>}(E) = \begin{pmatrix} -i[1 - f_K(E)]\Gamma_{MK,1} & 0 \\ 0 & -i[1 - f_K(E)]\Gamma_{MK,2} \end{pmatrix}. \quad (11c)$$

The lesser and greater Green's functions in this system can be derived by using the Keldysh formula

$$G^{<,>}(E) = G^r(E)\Sigma^{<,>}(E)G^a(E), \quad (12)$$

where

$$\Gamma_{MK,m} = 2\pi \sum_{k \in K} |V_{km}^{(MK)}|^2 \delta(E - \varepsilon_k), \quad m = 1, 2 \quad \text{and} \quad K = L, R \quad (13)$$

and $f_K(E)$, are the Fermi functions

$$f_K(E) = [\exp((E - \mu_K)/k_B T) + 1]^{-1}. \quad (14)$$

The Landauer formula for the electronic source-drain current (I_{sd}) is obtained from eqs (2)–(4). By summing over currents that arise from transfer of electrons and holes from the ground and excited molecular levels, respectively, I_{sd} then becomes

$$I_{sd} = \frac{1}{\hbar} \int_{-\infty}^{+\infty} \frac{dE}{2\pi} \sum_{m=1,2} \Gamma_{ML,m} G_{mm}^a(E) \Gamma_{MR,m} G_{mm}^a(E) [f_L(E) - f_R(E)]. \quad (15)$$

By including different couplings such as V_P and V_N , the final form of the self-energies will be given by [8]

$$\Sigma = \Sigma_{ML} + \Sigma_{MR} + \Sigma_P + \Sigma_{NL} + \Sigma_{NR}, \quad (16)$$

where Σ_{ML} and Σ_{MR} are the self-energies associated with the electron exchange between the molecule and the left lead and right lead, respectively. Σ_P is the self-energy associated with the coupling to the radiation field. Σ_{NL} and Σ_{NR} are the self-energies associated with the interaction between the molecular excitations and electron–hole pairs in the left and right metal leads, respectively. These self-energies on the Keldysh contour are

$$\Sigma_{MK}(\tau_1, \tau_2) = \begin{bmatrix} \Sigma_{MK,11}(\tau_1, \tau_2) & \Sigma_{MK,12}(\tau_1, \tau_2) \\ \Sigma_{MK,21}(\tau_1, \tau_2) & \Sigma_{MK,22}(\tau_1, \tau_2) \end{bmatrix}, \quad (17a)$$

$$\Sigma_{MK,mm'}(\tau_1, \tau_2) = \sum_{k \in K} V_{mk}^{(MK)} g_k(\tau_1, \tau_2) V_{km'}^{(MK)}, \quad (17b)$$

$$\Sigma_P(\tau_1, \tau_2) = i \sum_{\alpha} |V_{\alpha}^{(P)}|^2 \begin{bmatrix} F_{\alpha}(\tau_2, \tau_1) G_{22}(\tau_1, \tau_2) & 0 \\ 0 & F_{\alpha}(\tau_1, \tau_2) G_{11}(\tau_1, \tau_2) \end{bmatrix}, \quad (18)$$

$$\Sigma_{NK}(\tau_1, \tau_2) = \sum_{k \neq k' \in K} |V_{kk'}^{(NK)}|^2 g_k(\tau_1, \tau_2) g_{k'}(\tau_1, \tau_2) \begin{bmatrix} G_{22}(\tau_1, \tau_2) & 0 \\ 0 & G_{11}(\tau_1, \tau_2) \end{bmatrix}, \quad (19)$$

where g_k and f_{α} refer to free electron Green's function in the state k and the free photon Green's function of mode α , respectively.

Using the Langreth relations [10] we obtain the lesser and greater self-energies. The results become

$$\Sigma_P^<(E) = \sum_{\alpha} |V_{\alpha}^{(P)}|^2 \begin{bmatrix} (1 + N_{\alpha}) G_{22}^<(E + \omega_{\alpha}) & 0 \\ 0 & N_{\alpha} G_{11}^<(E - \omega_{\alpha}) \end{bmatrix}, \quad (20a)$$

$$\Sigma_P^>(E) = \sum_{\alpha} |V_{\alpha}^{(P)}|^2 \begin{bmatrix} N_{\alpha} G_{22}^>(E + \omega_{\alpha}) & 0 \\ 0 & (1 + N_{\alpha}) G_{11}^>(E - \omega_{\alpha}) \end{bmatrix}, \quad (20b)$$

where N_{α} is the number of photons in mode α , and eqs (20) were derived using the GFs of free photon field.

$$\begin{aligned} F_{\alpha}^<(\omega) &= -2\pi i N_{\alpha} \delta(\omega - \omega_{\alpha}), \\ F_{\alpha}^>(\omega) &= -2\pi i (1 + N_{\alpha}) \delta(\omega - \omega_{\alpha}). \end{aligned} \quad (21)$$

We can now perform summation over the interested α modes. For this purpose, only the pumping mode, $\alpha = 0$, is required, because molecule–radiation field coupling leads to pump one photon with $\alpha = 0$ and $N_0 = 1$, but for other states where $N_{\alpha \neq 0} = 0$, pumping is not possible.

Now, applying the Langreth rules [10] to eq. (19), we obtain the following expressions for the self-energies. The Langreth rule are as follows:

$$\begin{aligned} g_k^<(E) &= 2\pi i f_k(E) \delta(E - \varepsilon_k), \\ g_k^> &= -2\pi i [1 - f_k(E)] \delta(E - \varepsilon_k), \end{aligned}$$

where we use the definition of $g_k(\tau_1, \tau_2) = -i \langle T_c \hat{c}_k(\tau_1) \hat{c}_k^\dagger(\tau_2) \rangle$ in which T_c is the contour ordering operator. In eq. (19)

$$g_k(\tau_2, \tau_1) = -i \left\langle T_c \hat{c}_k(\tau_2) \hat{c}_k^\dagger(\tau_1) \right\rangle = i \left\langle \hat{c}_k^\dagger(\tau_1) \hat{c}_k(\tau_2) \right\rangle = g_k^<(\tau)$$

and

$$g_{k'}(\tau_1, \tau_2) = -i \left\langle T_c \hat{c}_{k'}(\tau_1) \hat{c}_{k'}^\dagger(\tau_2) \right\rangle = -i \left\langle \hat{c}_{k'}^\dagger(\tau_1) \hat{c}_{k'}(\tau_2) \right\rangle = g_{k'}^>(\tau_2).$$

Therefore, by replacing $g_k^<(E) = 2\pi i f_k(E) \delta(E - \varepsilon_k)$ and $g_{k'}^> = -2\pi i [1 - f_{k'}(E)] \delta(E - \varepsilon_{k'})$ and considering the fact that the maximum of $G^>$ and $G^<$ occur at $E - \omega$ and $E + \omega$, respectively we have

$$\begin{aligned} \Sigma_{\text{NK}}(E) &= \frac{1}{(2\pi)^2} \int d\omega dE \sum_{k \neq k' \in K} \left| V_{kk'}^{(\text{NK})} \right|^2 g_k^<(\tau_2) g_{k'}^>(\tau_2) \\ &\times \begin{bmatrix} G_{22}(\tau_1, \tau_2) & 0 \\ 0 & G_{11}(\tau_1, \tau_2) \end{bmatrix}. \end{aligned}$$

As a result we obtain

$$\Sigma_{\text{NK}}^<(E) = \int \frac{d\omega}{2\pi} B_{\text{NK}}(\omega, \mu_{\text{K}}) \begin{bmatrix} G_{22}^<(E + \omega) & 0 \\ 0 & G_{11}^<(E + \omega) \end{bmatrix}, \quad (22a)$$

$$\Sigma_{\text{NK}}^>(E) = \int \frac{d\omega}{2\pi} B_{\text{NK}}(\omega, \mu_{\text{K}}) \begin{bmatrix} G_{22}^>(E - \omega) & 0 \\ 0 & G_{11}^>(E - \omega) \end{bmatrix}, \quad (22b)$$

where μ_{K} refers to the electrochemical potential of the electrode $\text{K} = \text{L}, \text{R}$.

$$B_{\text{NK}}(\omega, \mu_{\text{K}}) = \int \frac{dE}{2\pi} C_{\text{NK}}(E, \omega) f_{\text{K}}(E) [1 - f_{\text{K}}(E + \omega)], \quad (23)$$

$$C_{\text{NK}}(E, \omega) = (2\pi)^2 \sum_{k \neq k' \in K} \left| V_{kk'}^{(\text{NK})} \right|^2 \delta(E - \varepsilon_k) \delta(E + \omega - \varepsilon_{k'}). \quad (24)$$

These expressions were obtained by the application of the free electron lesser and greater GFs for the electrodes, as given below.

$$\begin{aligned} g_k^<(E) &= 2\pi i f_{\text{K}}(E) \delta(E - \varepsilon_k); \\ g_k^>(E) &= -2\pi i [1 - f_{\text{K}}(E)] \delta(E - \varepsilon_k). \end{aligned} \quad (25)$$

Now by applying Keldysh method, various types of Green's functions appear, where the greater and lesser Green's functions are among these results. In this case greater Green's function, $g^>$, describes the propagation of excited electrons and the lesser Green's function, $g^<$, describes the occupied states from which electrons are excited.

The lesser and greater components of radiative contribution Σ_P are related to the lesser and greater components of GFs and become

$$\Sigma_{P0}^<(E) = |V_0^{(P)}|^2 \begin{bmatrix} 2G_{22}^<(E + \omega_0) & 0 \\ 0 & G_{11}^<(E - \omega_0) \end{bmatrix}, \quad (26a)$$

$$\Sigma_{P0}^>(E) = |V_0^{(P)}|^2 \begin{bmatrix} G_{22}^>(E + \omega_0) & 0 \\ 0 & 2G_{11}^>(E - \omega_0) \end{bmatrix}. \quad (26b)$$

To derive eq. (29), we apply the general expression (20) and consider only a single term $\alpha = 0$ and $N_0 = 1$. In the field of deriving spontaneous light emission flux, we use the frequency-resolved light emission (differential light emission flux) $I'_{em} = dI_{em}(\omega)/d\omega$. Thus the total integrated light emission is $I_{em}^{tot} = \int_0^\infty d\omega I'_{em}(\omega)$. Here, $I'_{em}(\omega)$ is derived from eq. (7) by considering $N_\alpha = 0$, using the self-energy (20) and summing over α which is confined to modes of frequency ω . Finally, we derive a more explicit form for eq. (20) and with $N_\alpha = 0$, it becomes

$$\Sigma_P^<(E) = \sum_\alpha |V_\alpha^{(P)}|^2 \begin{bmatrix} G_{22}^<(E + \omega_\alpha) & 0 \\ 0 & 0 \end{bmatrix} = \left(|V^{(P)}|^2 \right)_\omega \begin{bmatrix} G_{22}^<(E + \omega) & 0 \\ 0 & 0 \end{bmatrix}$$

in which

$$\gamma_P = 2\pi \sum_\alpha |V_\alpha^{(P)}|^2 \delta(\omega - \omega_\alpha)$$

and by considering the definition of

$$\rho_P(\omega) = \sum_\alpha \delta(\omega - \omega_\alpha) \Rightarrow \gamma_P = 2\pi |V^{(P)}|^2_\omega \rho_P(\omega)$$

and by replacing

$$|V^{(P)}|^2_\omega = \frac{\gamma_P}{2\pi \rho_P},$$

we, thus have,

$$\Sigma_P^<(E, \omega) = \frac{\gamma_P(\omega)}{2\pi \rho_P(\omega)} \begin{bmatrix} G_{22}^<(E + \omega) & 0 \\ 0 & 0 \end{bmatrix}. \quad (27a)$$

Using the same reasoning and argument, we have

$$\Sigma_P^>(E, \omega) = \frac{\gamma_P(\omega)}{2\pi \rho_P(\omega)} \begin{bmatrix} 0 & 0 \\ 0 & G_{11}^>(E - \omega) \end{bmatrix}, \quad (27b)$$

where

$$\gamma_P(\omega) = 2\pi \sum_\alpha |V_\alpha^{(P)}|^2 \delta(\omega - \omega_\alpha) = 2\pi \left(|V^{(P)}|^2 \right)_\omega \quad (28)$$

and $\rho_P(\omega)$ [11] denotes photon density of states given by

$$\rho_P(\omega) = \frac{\omega^2}{\pi^2 c^3}. \quad (29)$$

The differential light emission flux is derived from eq. (7) and it has the following form:

$$I'_{\text{em}}(\omega) = \rho_{\text{p}}(\omega) \int_{-\infty}^{+\infty} \frac{dE}{2\pi\hbar} \text{Tr}[\Sigma_{\text{p}}^{\leq}(E, \omega)G^{\gt}(E) - \Sigma_{\text{p}}^{\gt}(E, \omega)G^{\leq}(E)]. \quad (30)$$

Accordingly, the self-energies and the total light emission flux are given by

$$\Sigma_{\text{p}}^{\leq}(E) = \int_0^{\infty} d\omega \rho(\omega) \Sigma_{\text{p}}^{\leq}(E, \omega) = \begin{bmatrix} \int_0^{\infty} \frac{d\omega}{2\pi} \gamma_{\text{p}} G_{22}^{\leq}(E + \omega) & 0 \\ 0 & 0 \end{bmatrix}, \quad (31a)$$

$$\Sigma_{\text{p}}^{\gt}(E) = \int_0^{\infty} d\omega \rho(\omega) \Sigma_{\text{p}}^{\gt}(E, \omega) = \begin{bmatrix} 0 & 0 \\ 0 & \int_0^{\infty} \frac{d\omega}{2\pi} \gamma_{\text{p}} G_{11}^{\gt}(E - \omega) \end{bmatrix}, \quad (31b)$$

$$I_{\text{em}}^{\text{tot}} = \int_{-\infty}^{+\infty} \frac{dE}{2\pi\hbar} \text{Tr}[\Sigma_{\text{p}}^{\leq}(E)G^{\gt}(E) - \Sigma_{\text{p}}^{\gt}(E)G^{\leq}(E)]. \quad (32)$$

Considering the self-energies $\Sigma_{\text{NK}}^{\gt;\leq}(E)$ ($\text{K} = \text{L}, \text{R}$), eqs (22) are associated with energy transfer to electron-hole excitations in the metals. We shall focus, specially on $\Sigma_{\text{NK}}^{\leq}(E)$, eq. (22a); the treatment of $\Sigma_{\text{NK}}^{\gt}(E)$ goes along similar lines. In the wide band approximation, we assume that C_{NK} , eq. (24), is a constant. This implies that at $T \rightarrow 0$, the function B of eq. (23) is essentially a step function

$$B_{\text{NK}}(\omega, \mu_k) = C_{\text{NK}}\omega\Theta(\omega).$$

Using this result in (22a) we encounter integrals of the form $(2\pi)^{-1} \int_0^{\infty} d\omega \omega G_{22}^{\leq}(E + \omega)$ and $(2\pi)^{-1} \int_0^{\infty} d\omega \omega G_{11}^{\leq}(E + \omega)$, which can be approximated by $(2\pi)^{-1}(\varepsilon_2 - E) \int_0^{\infty} d\omega G_{22}^{\leq}(E + \omega)$ and $(2\pi)^{-1}(\varepsilon_1 - E) \int_0^{\infty} d\omega \omega G_{11}^{\leq}(E + \omega)$, respectively. The former of these integrals, i.e. the term involving G_{22}^{\leq} appears in $\Sigma_{\text{NK},11}^{\leq}$ and will appear in the expression that peaks near $E = \varepsilon_1$. We can, therefore, replace this term by its value for $E = \varepsilon_1$ and use $\int_{\varepsilon_1}^{\infty} d\omega G_{22}^{\leq}(\omega) \approx \int_{-\infty}^{\infty} d\omega G_{22}^{\leq}(\omega) = in_2$. The term involving G_{11}^{\leq} appears in $\Sigma_{\text{NK},22}^{\leq}$ and, therefore, its major contribution will be around $E = \varepsilon_2$. However, $\int_{\varepsilon_2}^{\infty} d\omega G_{11}^{\leq}(\omega) \approx 0$ because, even though $\int_{-\infty}^{\infty} d\omega G_{11}^{\leq}(\omega) = in_1$, most of the contribution comes from the neighbourhood of level 1, which is out of the boundary of the integral because it has ε_2 as its lower bound. We thus conclude that under our assumptions [8] the self-energy will be as follows:

$$\Sigma_{\text{NK}}^{\leq} \approx iB_{\text{NK}} \begin{pmatrix} n_2 & 0 \\ 0 & 0 \end{pmatrix}. \quad (33a)$$

Applying the same reasoning to Σ_{NK}^{\gt} , will yield

$$\Sigma_{\text{NK}}^{\gt} \approx -iB_{\text{NK}} \begin{pmatrix} 0 & 0 \\ 0 & 1 - n_1 \end{pmatrix}. \quad (33b)$$

The overall self-energy associated with this process, therefore, is $\Sigma_{\text{NK}}^{>,<} - \Sigma_{\text{NL}}^{>,<} + \Sigma_{\text{NR}}^{>,<}$, and will have the same form as the corresponding $\Sigma_{\text{NK}}^{>,<}$ with $B_{\text{N}} = B_{\text{NL}} + B_{\text{NR}}$ replacing B_{NK} . This result also implies that

$$\Gamma_{\text{NK}} = i (\Sigma_{\text{NK}}^{>} - \Sigma_{\text{NK}}^{<}) = B_{\text{NK}} \begin{pmatrix} n_2 & 0 \\ 0 & 1 - n_1 \end{pmatrix}. \quad (34)$$

Now we consider the self-energies $\Sigma_{\text{p}}^{>,<}$, eq. (31), associated with the coupling to the radiation field. These functions consist of integrals over ω , and the integrands contain products of $\gamma_{\text{p}}(\omega)$, a relatively weak function of ω , and $G_{mm}^{<,>}(E + \omega)$, $m = 1, 2$, that according to eq. (12) are products of a Lorentzian $G_{mm}^{\text{r}}(E \pm \omega)G_{mm}^{\text{a}}(E \pm \omega) = |G_{mm}^{\text{r}}(E \pm \omega)|^2$ and some function of energy $\Sigma^{<,>}(E)$.

The Lorentzian $|G_{mm}^{\text{r}}(E \pm \omega)|^2$ is peaked around $E \pm \omega = \varepsilon_m$, $m = 1, 2$. If the width of this function is small relative to the range over which $\gamma_{\text{p}}(\omega)$ varies with ω , we can then, replace

$$\Sigma_{\text{p},11}^{<}(E) = (2\pi)^{-1} \int_0^{\infty} d\omega \gamma_{\text{p}}(\omega) G_{22}^{<}(E + \omega),$$

in eq. (31a), by

$$(2\pi)^{-1} \gamma_{\text{p}}(\varepsilon_2 - E) \int_E^{\infty} d\omega G_{22}^{<}(\omega)$$

and

$$\Sigma_{\text{p},22}^{>}(E) = (2\pi)^{-1} \int_0^{\infty} d\omega \gamma_{\text{p}}(\omega) G_{11}^{>}(E - \omega)$$

by

$$(2\pi)^{-1} \gamma_{\text{p}}(E - \varepsilon_1) \int_E^{\infty} d\omega G_{11}^{>}(E - \omega).$$

Now, considering the fact that $G_{11}^{<}(E)$ picks around $E = \varepsilon_1$, it results in the same behaviour for $\Sigma_{\text{p},11}^{<}(E)$, because it enters the flux calculation only as a product with $G_{11}^{<}(E)$. Noting that $G_{22}^{<}(\omega)$ has a sharp peak near $\omega = \varepsilon_2$, we can now write

$$\begin{aligned} \Sigma_{\text{p},11}^{<}(\varepsilon_1) &= (2\pi)^{-1} \gamma_{\text{p}}(\varepsilon_{21}) \int_{\varepsilon_1}^{\infty} d\omega G_{22}^{<}(\omega) \\ &= (2\pi)^{-1} \gamma_{\text{p}}(\varepsilon_{21}) \int_{-\infty}^{\infty} d\omega G_{22}^{<}(\omega) = i \gamma_{\text{p}}(\varepsilon_{21}) n_2 \end{aligned}$$

where $n_2 = (2\pi i)^{-1} \int_{-\infty}^{\infty} dE G_{22}^{<}(E)$ is the population in level 2. Similarly, $\Sigma_{\text{p},22}^{>}(E)$ will be considerable only around $E = \varepsilon_2$ and therefore we have

$$\Sigma_{\text{p},22}^{>}(\varepsilon_2) = (2\pi)^{-1} \gamma_{\text{p}}(\varepsilon_{21}) \int_0^{\infty} d\omega G_{11}^{>}(\varepsilon_2 - \omega) = (2\pi)^{-1} \gamma_{\text{p}}(\varepsilon_{21}) \int_{-\infty}^{\varepsilon_2} d\omega G_{11}^{>}(\omega),$$

where, again, the upper integration limit can be set to ∞ yielding

$$\Sigma_{\text{p},22}^{>}(\varepsilon_2) = (2\pi)^{-1} \gamma_{\text{p}}(\varepsilon_{21}) \int_{-\infty}^{\infty} d\omega G_{11}^{>}(\omega) = -i \gamma_{\text{p}}(\varepsilon_{21}) (1 - n_1),$$

in which, we have used for the population n_1 of level 1 the density $1 - n_1 = - (2\pi i)^{-1} \int_{-\infty}^{\infty} dE G_{11}^>(E)$. We thus find that for our present application we can use [8]

$$\Sigma_P^<(E) = i\gamma_P(\varepsilon_{21}) \begin{bmatrix} n_2 & 0 \\ 0 & 0 \end{bmatrix}, \quad (35a)$$

$$\Sigma_P^>(E) = -i\gamma_P(\varepsilon_{21}) \begin{bmatrix} 0 & 0 \\ 0 & 1 - n_1 \end{bmatrix}, \quad (35b)$$

$$\Gamma_P = i(\Sigma_P^> - \Sigma_P^<) = \gamma_P(\varepsilon_{21}) \begin{bmatrix} n_2 & 0 \\ 0 & 1 - n_1 \end{bmatrix}. \quad (36)$$

In eqs (33)–(36), n_1 and n_2 denote occupations of the HOMO and LUMO states of the nanowire, respectively. These parameters are defined as

$$in_m = \int \frac{dE}{2\pi} G_{mm}^<(E) \quad \text{or} \quad -i(1 - n_m) = \int \frac{dE}{2\pi} G_{mm}^>(E), \quad m = 1, 2. \quad (37)$$

3. Optical flux (fluorescence)

In this section we study the dependence of optical flux (light emission which is induced by electronic current) on the gate voltage and temperature in biased voltage. The radiation fluxes are related to the radiation field coupling through Σ_P [8] by the following relation:

$$\begin{aligned} I'_{em}(\omega) &= \rho_P(\omega) \int_{-\infty}^{+\infty} \frac{dE}{2\pi\hbar} [\Sigma_{P,11}^<(E, \omega)G_{11}^>(E) - \Sigma_{P,11}^>(E, \omega)G_{11}^<(E)] \\ &= -\rho_P(\omega) \int_{-\infty}^{+\infty} \frac{dE}{2\pi\hbar} [\Sigma_{P,22}^<(E, \omega)G_{22}^>(E) - \Sigma_{P,22}^>(E, \omega)G_{22}^<(E)]. \end{aligned} \quad (38)$$

The total light emission is then,

$$\begin{aligned} I_{em}^{tot} &= \int_0^{\infty} d\omega I'_{em}(\omega) \\ &= \int_{-\infty}^{+\infty} \frac{dE}{2\pi\hbar} [\Sigma_{P,11}^<(E)G_{11}^>(E) - \Sigma_{P,11}^>(E)G_{11}^<(E)] \\ &\quad - \int_{-\infty}^{+\infty} \frac{dE}{2\pi\hbar} [\Sigma_{P,22}^<(E)G_{22}^>(E) - \Sigma_{P,22}^>(E)G_{22}^<(E)]. \end{aligned} \quad (39)$$

The values taken for the parameters are: $\Gamma_{MK,m} = 0.1$ eV ($K = L, R; m = 1, 2$), $\gamma_P = 10^{-6}$ eV and $B_{NL} = B_{NR} = 0.1$ eV [8], where $\Gamma_{MK,m}$ is the damping rates associated with electron transfer from HOMO level ($m = 1$) or LUMO level ($m = 2$) to the left or right lead, γ_P is the radiative width, B_{NL}, B_{NR} are the damping rates associated with energy transfer to electron–hole pairs in the left lead and right lead, respectively.

Here, we also study the effects of asymmetric connections between nanowire and electrodes. The electrochemical potentials in the left and right electrodes are

$$\mu_L = E_F + \eta eV$$

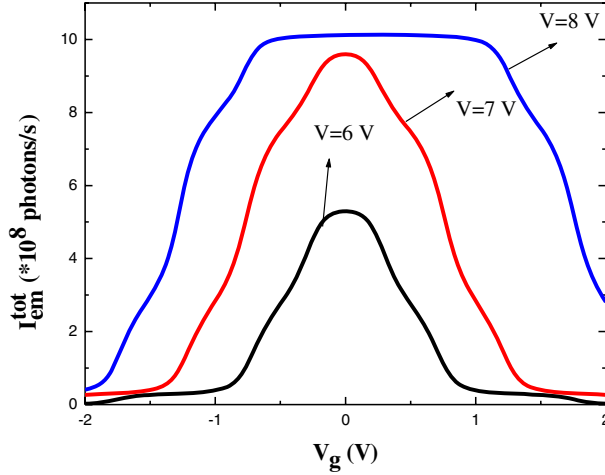


Figure 1. Light emission vs. gate voltage in the symmetric connections to the electrodes with constant temperature ($T = 300$ K) at $V = 8$ V (blue line), $V = 7$ V (red line) and $V = 6$ V (black line).

and

$$\mu_R = E_F - (1 - \eta)eV,$$

where η and E_F are the division factor and Fermi energy, respectively. This asymmetry affects the damping rate parameters Γ_M and B_N . We define $\Gamma_{ML,m} = (1 - \eta)\Gamma_M$, $\Gamma_{MR,m} = \eta\Gamma_M$; $m = 1, 2$ and $B_{NL} = (1 - \eta)B_N$, $B_{NR} = \eta B_N$ [8].

The gate voltage-dependent response for symmetric connection of the nanowire to the electrodes is plotted in figure 1. As can be seen, by increasing the bias voltage at constant gate voltage, the emission flux enhances. The reason for this behaviour is given as follows: Due to the coupling of electrons from the LUMO with holes in the HOMO, excitons are created. By increasing the biased voltage, the number of electrons which enter from electrodes increases. This, in turn, causes an increase in the number of photons which are produced from the recombination of excitons. These curves show optimum operation at $V_g = 0$ V.

As seen from figure 2, when the nanowire is connected to the electrodes asymmetrically, light emission curves are asymmetric with respect to the gate voltage. Each curve has its special optimum gate voltage that differs from the other curves. With increasing η the fluorescence becomes greater and the peak becomes broader. We know that electrons are transported from LUMO and holes are transported from HOMO and enhancement of fluorescence show that LUMO and HOMO of the nanowire are matched to the Fermi level of electrodes better than when the nanowire is connected to the electrodes symmetrically. In this work, by connecting the electrodes to the nanowire asymmetrically, this matching is improved.

As can be seen from figure 2, in the symmetric connection at $V_g = 0$ V the radiation flux has its maximum value. Therefore, to plot temperature-dependent behaviour of I_{em}^{tot} we set $V_g = 0$ V. The temperature dependence of I_{em}^{tot} is plotted in figure 3 for different values of η and the ascending behaviour seen with respect to the temperature is observed. This

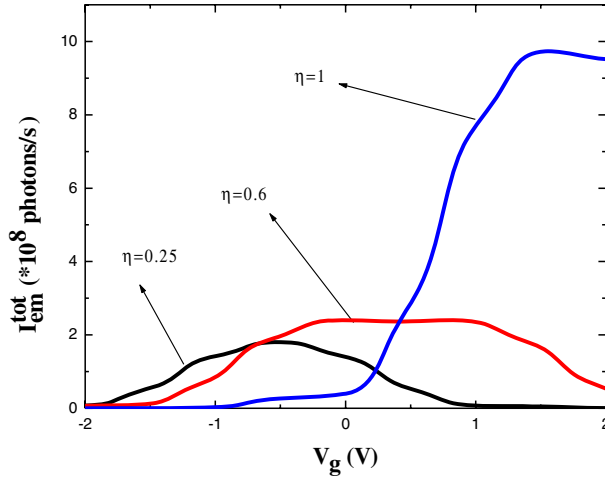


Figure 2. Fluorescence light emission from the nanowire as a function of V_g in the asymmetric connections and with constant V ($V = 4$ V) and T ($T = 300$ K) at $\eta = 1$ (blue line), $\eta = 0.6$ (red line), $\eta = 0.25$ (black line).

behaviour is in agreement with the temperature-dependent curve of photoluminescence for PbS nanocrystals [12].

4. Electronic source-drain current

The electronic source-drain current flows through the system (matter) due to different reasons such as magnetism, applied voltage or field radiations. These, in turn, lead to various effects such as rectification, switching, Coulomb blockade.

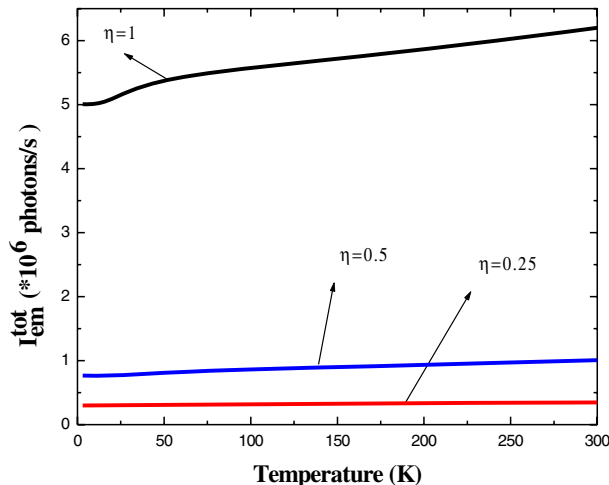


Figure 3. Temperature-dependent curves for light emission in the asymmetric connections with constant V ($V = 0.5$ V) and V_g ($V_g = 0$ V) at $\eta = 1$ (black line), $\eta = 0.5$ (blue line), $\eta = 0.25$ (red line).

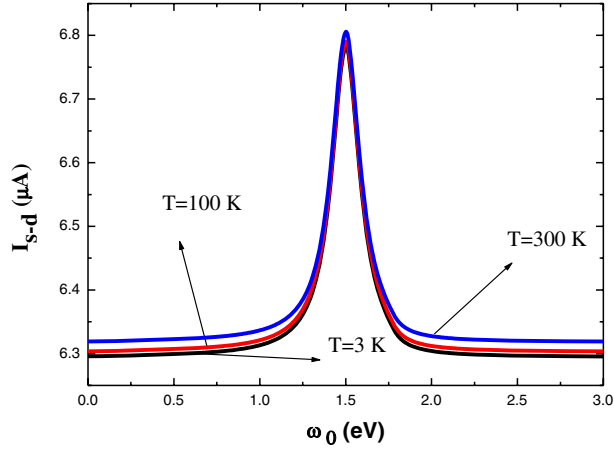


Figure 4. Electronic source-drain current for different temperatures as a function of incident photon energy in the symmetric connections with constant V_g ($V_g = 1$ V) and V ($V = 3$ V) at $T = 300$ K (blue line), $T = 100$ K (red line), $T = 3$ K (black line).

The electronic source-drain current can be obtained from eq. (7) by replacing $\Sigma_B^{<>}$ with either $\Sigma_{ML}^{<}$ or $\Sigma_{MN}^{<}$. Thus, this current becomes [8]

$$\begin{aligned}
 I_{sd} &= \int_{-\infty}^{+\infty} \frac{dE}{2\pi\hbar} \text{Tr}[\Sigma_{ML}^{<}(E)G^{>}(E) - \Sigma_{ML}^{>}(E)G^{<}(E)] \\
 &= - \int_{-\infty}^{+\infty} \frac{dE}{2\pi\hbar} \text{Tr}[\Sigma_{MR}^{<}(E)G^{>}(E) - \Sigma_{MR}^{>}(E)G^{<}(E)].
 \end{aligned} \tag{40}$$

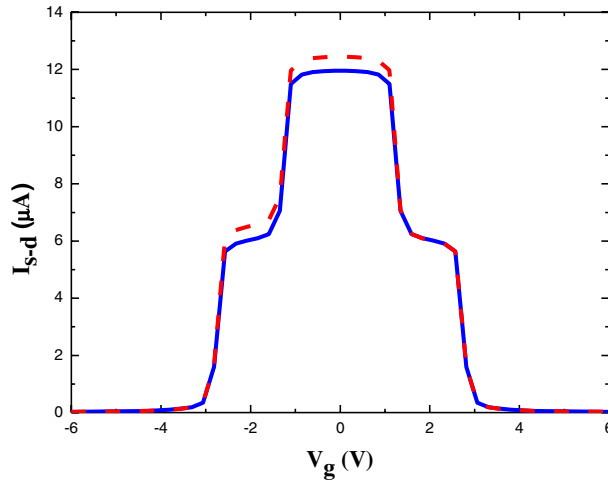


Figure 5. Electronic source-drain current in the symmetric connections vs. gate voltage with constant V ($V = 7$ V) and T ($T = 300$ K) at $\omega = 0$ eV (blue line), $\omega = 1.5$ eV (red line).

The values for the parameters used are as follows: $\gamma_p = 10^{-6}$ eV, $B_{NL} = B_{NR} = 0.1$ eV, $\Gamma_{ML,1} = \Gamma_{MR,1} = 0.01$ eV, $\Gamma_{ML,2} = \Gamma_{MR,2} = 0.2$ eV [8], where $\Gamma_{ML,1}$ and $\Gamma_{MR,1}$ are damping rates associated with electron transfer from HOMO level to the left lead and right lead, respectively and $\Gamma_{ML,2}$ and $\Gamma_{MR,2}$ are damping rates associated with electron transfer from LUMO level to the left lead and right lead, respectively. As can be seen from figure 4, the maximum value of current occurs in $\omega_0 = 1.5$ eV which equals to the assumed HOMO–LUMO gap.

As temperature increases, the current I_{sd} will also increase because the nanowire is a semiconductor and the temperature rise leads to the increase of carrier density. Figure 5 shows that maximum value of I_{sd} at $V_g = 0$. In this case, increasing the gate voltage leads to decrease of I_{sd} , i.e., gate voltage controls the current. The observation of such a behaviour has been reported by several researchers [13–15]. Also radiation of light on the nanowire generates current which is due to the transfer of electrons from HOMO to LUMO and increasing the free electron density.

5. Conclusion

In this study we presented an investigation on the photoinduced current and optical flux in a system of electrode/nanowire/electrode in the temperature range between 3 and 300 K. We used the Green's function approach and Keldysh formalism for our study and investigated the effects of different parameters such as bias voltage, gate voltage, temperature and incident light energy on the performance of the system. The model system under consideration was a semiconducting nanowire which was sandwiched between two one-dimensional semi-infinite metallic electrodes in the presence of gate voltage and source-drain bias voltage. Our calculations showed that both the photoinduced current and light emission induced by electronic current have similar temperature dependencies. The increase in temperature on the one hand, and the electron–photon interaction of the incident light, on the other hand, cause more electron transfer from HOMO to LUMO in the nanowire semiconductor. Therefore, we saw an increase in the photoinduced current. Our results are in agreement with the experimental data. We also studied the effects of symmetric and asymmetric connections of the nanowire to the electrodes. In particular we showed that with asymmetric connections to the electrodes, we could control height and broadening of the emission peak. Broadening of emission peak is an indication of the broadening of HOMO or LUMO levels which is due to the application of the gate voltage. In addition, our calculation showed that, in the presence of gate voltage, the source-drain current is quantized.

References

- [1] N S Sariciftci, L Smilowitz, A J Heeger and F Wudl, *Science* **258**, 1474 (1992)
- [2] J De la Torre, A Souia, M Lemiti, A Poncet, C Busseret, G Guillota, G Bremond, O Gonzalez, B Garrido and J R Morante, *Physica E* **17**, 604 (2003)
- [3] V M Shalaev, *Phys. Rev. B* **53**, 11388 (1996)
- [4] F T Vasko and O Keller, *Phys. Rev. B* **58**, 15666 (1998)
- [5] V Ya Degoda and A O Sofienko, *Physica B* **426**, 24 (2013)

- [6] M Choe *et al*, *Appl. Phys. Lett.* **103**, 223305 (2013)
- [7] M C Jeong, B Y Oh, M H Ham and J M Myoung, *Appl. Phys. Lett.* **88**, 202105 (2006)
- [8] M Galperinand and A Nitzan, *J. Chem. Phys.* **124**, 234709 (2006)
- [9] A Saffarzadeh, *J. Appl. Phys* **103**, 083705 (2008)
- [10] D C Langreth, *Linear and nonlinear electron transport in solids* (Plenum Press, 1976)
- [11] O Sveito, *Principles of lasers* (Plenum Press, 1982)
- [12] M N Nordin, J Li, S K Clowes and R J Curry, *Nanotechnol.* **23**, 275701 (2012)
- [13] J Kong, N R Franklin, C Zhou, M G Chapline, S Peng, K Cho and H Dai, *Science* **287**, 622 (2000)
- [14] M Egginger, S Bauer, R Schwödiauer, H Neugebauer and N S Sariciftci, *Monatsh Chem.* **140**, 735 (2009)
- [15] B Xu, X Xiao, X Yang, L Zang and N Tao, *J. Am. Chem. Soc.* **127**, 2386 (2005)